Cooling of a newborn compact star with a QCD phase transition

K. -W. Wong*

*Department of Physics, The Chinese University of Hong Kong, Shatin, New Territories, Hong Kong, China
and Department of Astronomy, University of Virginia, PO Box 3818, Charlottesville, Virginia 22903, USA*

M. -C. Chu[†]

Department of Physics, The Chinese University of Hong Kong, Shatin, New Territories, Hong Kong, China

We study the cooling behavior of an isolated strange-quark star, using an equation of state derived from perturbative QCD up to second order in a strong coupling constant, and we compare it with that of a neutron star. After an initial rapid cooling, a quark star may undergo the QCD phase transition to become a neutron star. We propose several signatures for such a scenario: a large amount of energy can be released due to latent heat, a long duration γ-ray source, and a second neutrino burst after a supernova explosion.

I. INTRODUCTION

The Witten proposal that symmetric deconfined u, d, and s-quark matter may be the absolute ground state of matter [1] has aroused much interest, and the properties of strange stars have been widely studied since then. An important question is whether the observed compact stars are neutron stars or strange stars, which are made up of deconfined u, d, and s quarks. With the launching of the new generation of x-ray detectors Chandra and XMM, it has become possible now to have an accurate measurement of the radii and surface temperature of compact stars [2–5]. However, theoretical calculations using the MIT Bag Model equation of state (EOS) show that the mass and size of a strange star are comparable to those of a neutron star [6,7]. Hence it is important to identify other observables that can be used to distinguish a strange star from a neutron star. One possibility is to study the cooling of an isolated compact star. The cooling curves of quark matter and neutron matter are found to be significantly different due to the difference in their thermal properties and energy loss mechanisms [7–11].

In this paper, we study the effects of the QCD phase transition on the cooling of a compact star and possible signatures of the quark phase. Regardless of the validity of Witten's proposal, the formation of quark-gluon plasma should be favored in high temperature and density [12]; we therefore suggest that a strange-quark star may be formed just after a supernova explosion, in which both conditions may be satisfied [13]. Because the initial temperature is so high [14] $T_i \sim 40$ MeV, the initial compact star is likely to be a bare strange star [10]. When it cools down to the phase transition temperature T_p, the quark matter may become energetically unstable compared to nuclear matter, and the strange star will convert to a

neutron star. During the phase transition, a large amount of latent heat, of the order of 10^{53} erg, can be released, which can be a possible energy source of gamma-ray bursts (GRB's).

The latest lattice QCD calculations of T_p [15,16] indicate, though with relatively large uncertainties at high chemical potential, that T_p drops from its zero density value of 140 MeV to about 50 MeV at 1.5 times nuclear matter density $\rho_0 = 0.17$ fm^{-3} and down to a few MeV for density a few times ρ_0. Some previous proto-neutron star evolution calculations indeed show that it is feasible to reach the phase transition in supernovae [17]. While there are still large uncertainties in both high density QCD and the proto-neutron star evolution, we believe it is worthwhile to study the possible consequences of the QCD phase transition in supernovae. We assume a constant T_p in density throughout the star and present results for $T_p = 1$, 10 MeV for comparison. We adopt the simple picture that matter at temperature above (below) T_p is in the quark (hadronic) phase.

It has been argued that the rapid cooling of strange stars by pion and $e^- e^+$ pair production can be a power source of GRB's [8–11]. However, if the QCD phase transition is not considered, the temperature of the compact star drops rapidly and the duration of the burst—being less than 10^{-2} s—is too short to account for long duration GRB's. In our model, the star stays at the phase transition temperature for a relatively long time, and the photon luminosity is maintained in the range 10^{48}–10^{54} erg s^{-1} with duration 10^{-3} s up to 10^4 s (or even longer), which is consistent with both long and short GRB's. Thus the latent heat may solve the problem of the energy supply of GRB's.

Another signature of quark stars that has been discussed is the relatively low luminosity of γ rays when the quark star cools down [11]. Our model shows that the luminosity in the γ-ray range can be as high as 10^{38-39} erg s^{-1} with a very long duration of $\sim 10^{13-14}$ s,

*Electronic address: kwwong@virginia.edu
[†]Electronic address: mcchu@phy.cuhk.edu.hk

which is much longer than the case considered by Page and Usov [11]. The satellite Integral launched recently is just sensitive to γ rays in the energy range of interest. If a long duration γ-ray source is detected, it could be a signature of the phase transition [18,19].

A remarkable feature of a strange star to neutron star phase transition is the emission of a second neutrino burst after the supernova explosion. A similar scenario was also proposed in Aguilera *et al.*'s work [20], but with a different physical mechanism. In our model, the burst is due to the phase transition from a quark star to a neutron star, which has a higher neutrino emissivity. In Aguilera *et al.*'s work, the burst is due to the trapping of neutrinos when the temperature is high, which are then released suddenly when the quark star cools. Nevertheless, both works suggest that a second neutrino burst is a signature of the existence of quark stars.

This paper is organized as follows. Section II describes the EOS used in the quark phase. The stability of the strange-quark star is investigated in Sec. III. The effect of strange-quark mass is studied in Sec. IV. We describe how to calculate the cooling history and phase transition of compact stars in Secs. V and VI. Section VII describes the models we used. The calculated results for the various models are presented in Sec. VIII. Section IX is a short discussion and summary of our work.

II. COLD EQUATION OF STATE FROM PERTURBATIVE QCD

Various EOS's have been used to study the properties of strange stars. The most widely used one is the MIT Bag Model due to its simple analytic form [6]. It has been pointed out that it is difficult to distinguish the strange stars described by the MIT Bag Model from neutron stars due to the similarities in their maximum mass $\sim 2M_\odot$ ($M_\odot$ is a solar mass) and radius ~ 10 km [21]. On the other hand, Fraga *et al.* [21] studied quark star structure by using the EOS of perturbative QCD for cold, dense quark matter up to order α_s^2, using a modern determination of the running of the coupling constant. Their results show that strange stars can have a radius of about 5.8 km and a mass of a typical neutron star, and such a small compact star can actually be distinguished from neutron stars. Since the strong coupling constant becomes small in the high density limit, perturbative QCD may be a fair description of matter in the interior of a compact star. Hence we follow Fraga's work and examine in detail the conditions of absolute and global stability of strange-quark stars, as well as the effects of strange-quark mass. It has been argued that perturbative QCD may fail to describe the matter at the surface of a strange star due to the strong coupling at low density. However, the main structure of a compact star is determined by matter properties in the high density regime. Moreover, it

is worthwhile to study the dependence of compact star properties on models of EOS.

The chemical equilibrium of strange-quark matter is maintained by the weak-interaction reactions:

$$d \leftrightarrow u + e + \overline{\nu}_e, \tag{1}$$

$$s \leftrightarrow u + e + \overline{\nu}_e \tag{2}$$

and

$$s + u \leftrightarrow u + d. \tag{3}$$

Given the thermodynamic potential of each species $\Omega_i (i = u, d, s, e)$, the number densities can be obtained from the thermodynamic relation:

$$n_i = -\frac{\partial \Omega_i}{\partial \mu_i}, \tag{4}$$

where μ_i is the chemical potential. The conditions of chemical equilibrium are

$$\mu_d = \mu_u + \mu_e, \tag{5}$$

$$\mu_d = \mu_s. \tag{6}$$

Together with the charge neutrality condition:

$$\tfrac{2}{3} n_u - \tfrac{1}{3}(n_d + n_s) - n_e = 0, \tag{7}$$

the thermodynamic properties will be determined by one independent choice of chemical potential only, which we have chosen to be $\mu \equiv \mu_d = \mu_s$ in our calculations. The total pressure is given by

$$P(\mu) = -\sum_i \Omega_i(\mu), \tag{8}$$

and the total energy density is

$$\epsilon(\mu) = \sum_i [\Omega_i(\mu) + \mu_i(\mu) n_i(\mu)]. \tag{9}$$

At the zero quark mass limit, $\Omega_u = \Omega_d = \Omega_s$ implying $n_u = n_d = n_s$. Hence the charge neutrality condition is automatically satisfied, without any need of electrons. The perturbative QCD thermodynamic potential at zero temperature has been calculated up to order α_s^2 [22,23], which in the modified minimal subtraction scheme [23] is

$$\Omega(\mu) = -\frac{N_f \mu^4}{4\pi^2} \left\{ 1 - 2\left(\frac{\alpha_s}{\pi}\right) - \left[G + N_f \ln\left(\frac{\alpha_s}{\pi}\right) \right. \right.$$
$$\left. \left. + \left(11 - \frac{2}{3}N_f\right) \ln\frac{\Lambda}{\mu} \right] \left(\frac{\alpha_s}{\pi}\right)^2 \right\}, \tag{10}$$

where $G = G_0 - 0.536 N_f + N_f \ln N_f$, $G_0 = 10.374 \pm 0.13$, N_f is the number of quark flavors, Λ is the renormalization subtraction point, and

$$\alpha_s(\Lambda) = \frac{4\pi}{\beta_0 u}\left[1 - \frac{2\beta_1}{\beta_0^2}\frac{\ln(u)}{u} + \frac{4\beta_1^2}{\beta_0^4 u^2}\left(\left(\ln(u) - \frac{1}{2}\right)^2\right.\right.$$
$$\left.\left. + \frac{\beta_2\beta_0}{8\beta_1^2} - \frac{5}{4}\right)\right], \tag{11}$$

with $u = \ln(\Lambda^2/\Lambda_{\overline{MS}}^2)$, $\beta_0 = 11 - 2N_f/3$, $\beta_1 = 51 - 19N_f/3$, and $\beta_2 = 2857 - 325N_f^2/27$. The boundary condition of $\alpha_s = 0.3089$ at $\Lambda = 2$ GeV for $N_f = 3$ gives $\Lambda_{\overline{MS}} = 365$ MeV.

All the thermodynamic properties can be obtained from the thermodynamic potential if Λ is fixed. It is believed that Λ/μ lies in the range between 2 and 3 [21]. Figure 1 shows the total pressure of strange-quark matter relative to the pressure of an ideal gas, P_0, as a function of the chemical potential μ. Both the first and second order terms decrease the pressure of the strange-quark matter relative to the ideal gas. It has been pointed out that using perturbation theory at zero pressure is invalid [21]. Numerical calculation shows that at zero pressure, α_s/π lies between 0.207 and 0.191, which is less than 1 if Λ/μ lies between 2 and 3. The EOS's for $\Lambda/\mu = 2.473$, 2.88, and free gas are shown in Fig. 2. It turns out that this EOS is very similar to the MIT Bag Model EOS, with an effective Bag constant [21], and we would have obtained basically the same results using the latter. None of our results in the cooling calculation depends on the validity of perturbative QCD in the compact star regime.
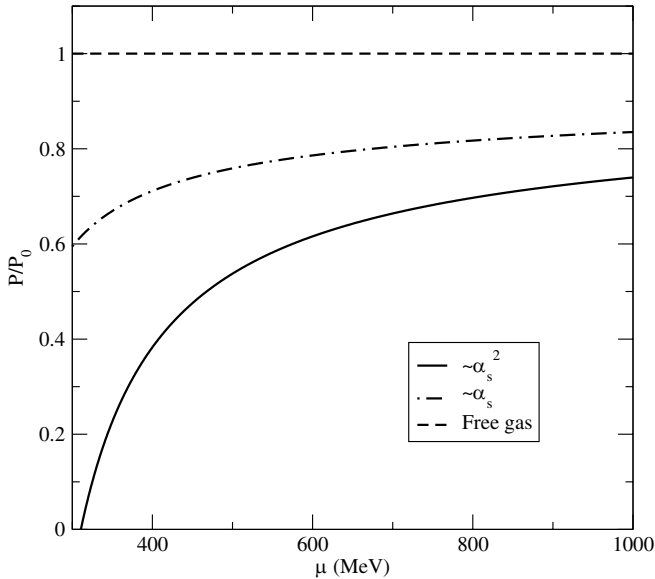

FIG. 1. The total pressure of strange-quark matter, P, relative to the pressure of an ideal gas, P_0, as a function of chemical potential, μ. P is calculated up to first and second order in strong coupling constant, α_s. Here we take $\Lambda = 2.88\mu$ and zero quark mass approximation [21].
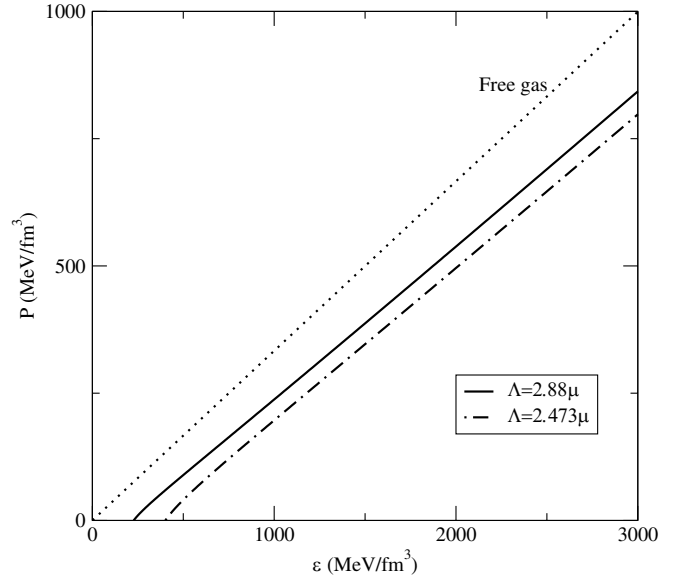

FIG. 2. Equation of state (pressure, P, vs energy density, ϵ) for cold quark matter with massless quark approximation at various Λ and free gas [21].

III. STABILITY OF STRANGE-QUARK MATTER

A strong condition for strange-quark matter to be the absolute ground state of cold matter is that the energy per baryon at zero pressure $\mathcal{E}_Q(0)$ is less than that of ^{56}Fe:

$$\mathcal{E}_Q(0) < \mathcal{E}_{\text{Fe}} = 930.4 \text{ MeV}. \tag{12}$$

The upper panel of Fig. 3 shows that strange-quark matter is absolutely stable for $\Lambda \gtrsim 2.88\mu$. At $\Lambda = 2.88\mu$, the baryonic number density at zero pressure is about $1.52n_0$, where n_0 is the normal nuclear matter number density. Therefore, strange-quark matter can be the true ground state, and bare strange stars can exist if $\Lambda \gtrsim 2.88\mu$.

A weaker condition for strange-quark matter to be stable is that the average energy per baryon of the bulk matter is less than that of ^{56}Fe, i.e., the binding energy per baryon of the bulk strange-quark matter $\mathcal{E}_{\text{binding}}(\text{SS})$ is larger than that of ^{56}Fe, $\mathcal{E}_{\text{binding}}(\text{Fe})$:

$$\mathcal{E}_{\text{binding}}(\text{SS}) = \frac{M_B - M_G}{A} > \mathcal{E}_{\text{binding}}(\text{Fe}) = 8.525 \text{ MeV}, \tag{13}$$

where M_B and M_G are the baryonic mass and gravitational mass of strange-quark matter, respectively, which are to be calculated by the Tolman-Oppenheimer-Volkov equations. We have plotted the binding energy per baryon of the maximum mass star against Λ in the lower panel of Fig. 3. We found that the strange star can be globally stable compared to iron at infinity if $\Lambda > 2.35\mu$.

The weak stability condition above overestimates the stability of a strange star, since the gravitational binding of bulk ^{56}Fe matter is ignored. A fairer condition is to
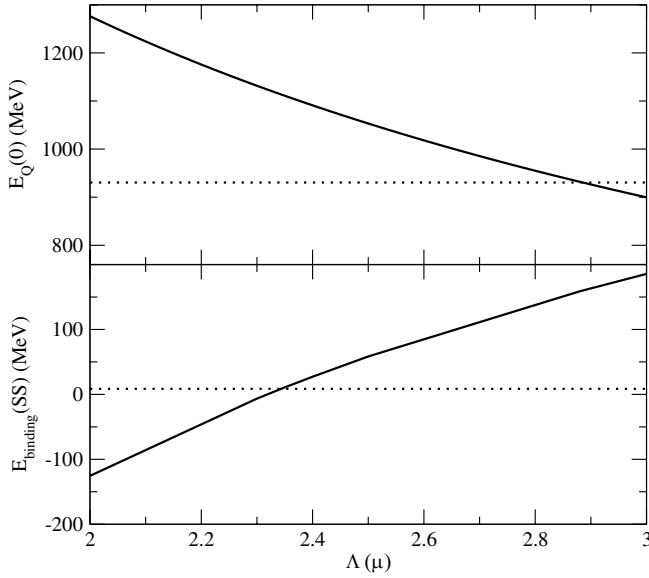
FIG. 3. Upper panel: Energy per baryon at zero pressure, $\mathcal{E}_Q(0)$, as a function of Λ/μ. The dotted line corresponds to the energy per baryon of ^{56}Fe, which is equal to 930.4 MeV. Absolute stability of strange-quark matter corresponds to $\Lambda \geq 2.880\mu$. Lower panel: Binding energy per baryon $\mathcal{E}_{\mathrm{binding}}$(SS) as a function of Λ/μ. The dotted line corresponds to the binding energy of Fe, which is equal to 8.525 MeV. Global stability corresponds to $\Lambda/\mu \geq 2.35\mu$.

compare the binding energy of a strange star with that of a neutron star. There are inevitably some dependences on the EOS's used in such a comparison. In Fig. 4 we show the parameter regime in which strange stars are more stable than neutron stars using one particular EOS (HV). We have used several other EOS's to reach a similar conclusion that strange stars are more stable than neutron stars for $\Lambda \gtrsim 2.7\mu$ (Table I).
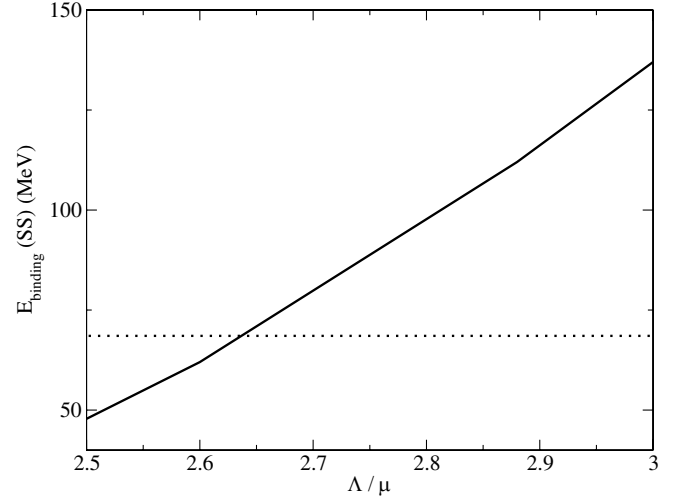

FIG. 4. Binding energy per baryon $\mathcal{E}_{\mathrm{binding}}$(SS) as a function of Λ/μ for baryonic mass of strange stars being equal to that of a $1.4M_\odot$ neutron star with HV EOS. The dotted line corresponds to the binding energy per baryon of the neutron star, which is equal to 68 MeV. Global stability compared to the neutron star corresponds to $\Lambda \geq 2.65\mu$.

IV. EFFECT OF MASSIVE STRANGE QUARKS

In the density range of a quark star, i.e., chemical potential $\sim$300–600 MeV, the strange-quark mass ($\sim$ 150 MeV) may alter the EOS. We consider the correction of the thermodynamic potential due to strange-quark mass m_s up to first order in α_s. The masses of u and d quarks are small and can be neglected. The individual thermodynamic potentials are [7]

$$\Omega_f(\mu_f) = -\frac{\mu_f^4}{4\pi^2}\left\{1 - 2\left(\frac{\alpha_s}{\pi}\right) - \left[G + N_f \ln\left(\frac{\alpha_s}{\pi}\right) + \left(11 - \frac{2}{3}N_f\right)\ln\frac{\Lambda}{\mu}\right]\left(\frac{\alpha_s}{\pi}\right)^2\right\}, \tag{14}$$

$$\Omega_s(\mu_s) = -\frac{1}{4\pi^2}\left\{\mu_s(\mu_s^2 - m_s^2)^{1/2}\left(\mu_s^2 - \frac{5}{2}m_s^2\right) + \frac{3}{2}m_s^4 \ln\left(\frac{\mu_s + (\mu_s^2 - m_s^2)^{1/2}}{m_s}\right) - 2\left(\frac{\alpha_s}{\pi}\right)\left[3\left(\mu_s(\mu_s^2 - m_s^2)^{1/2}\right.\right.\right.$$
$$- m_s^2 \ln\left(\frac{\mu_s + (\mu_s^2 - m_s^2)^{1/2}}{m_s}\right)\right)^2 - 2(\mu_s^2 - m_s^2)^2 - 3m_s^4\ln^2\left(\frac{m_s}{\mu_s}\right) + 6\ln\left(\frac{\sigma}{\mu_s}\right)\left(\mu_s m_s^2(\mu_s^2 - m_s^2)^{1/2}\right.$$
$$\left.\left.- m_s^4 \ln\left(\frac{\mu_s + (\mu_s^2 - m_s^2)^{1/2}}{m_s}\right)\right)\right] - \mu^4\left[G + N_f \ln\left(\frac{\alpha_s}{\pi}\right) + \left(11 - \frac{2}{3}N_f\right)\ln\frac{\Lambda}{\mu}\right]\left(\frac{\alpha_s}{\pi}\right)^2\right\}, \tag{15}$$

$$\Omega_e(\mu_e) = -\frac{\mu_e^4}{12\pi^2}, \tag{16}$$

where $f = u$ or d, and σ is the renormalization point for the strange-quark mass. It is found that a suitable choice for σ is 313 MeV[25].

The EOS's are calculated for $\Lambda = 2.473$, 2.88, and various m_s numerically (Fig. 5) [26]. For

$m_s \leq 225$ MeV, the changes in pressure compared to massless EOS are less than $\sim$5% in the high energy density limit. In the low energy density limit, the changes are significant because the strange-quark mass is not small compared to the chemical potentials. Since the global structure of a compact star is mainly determined by the high density regime—about several times the normal nuclear energy density—of the EOS, the effect

TABLE I. Binding energy, $\mathcal{E}_{\text{binding}}$, for various compact stars. A neutron star gravitational mass $M_G(\text{NS}) = 1.4M_\odot$ is assumed, and the baryonic masses of strange stars are chosen to be equal those of the neutron stars. The many-body approximation for HV, HFV, $\Lambda_{\text{BroB}}^{\text{RBHF}}$ + HFV, and $G_{\text{M78}}^{\text{K240}}$ EOS's are relativistic Hartree, relativistic Hartree-Fock, relativistic Brueckner-Hartree-Fock + relativistic Hartree-Fock, and relativistic Hartree, respectively [24].

		$\mathcal{E}_{\text{binding}}(\text{NS})$			$\mathcal{E}_{\text{binding}}(\text{SS})$
EOS (NS)	$M_B/M_\odot$	(MeV)	Λ/μ	$M_G(\text{SS})/M_\odot$	(MeV)
HV	1.51	68.4	2.473	1.44	43.5
HV	1.51	68.4	2.600	1.41	62.1
HV	1.51	68.4	2.880	1.33	111.9
HV	1.51	68.4	3.000	1.29	136.8
HFV	1.60	117.4	2.473	1.516	49.3
HFV	1.60	117.4	2.600	1.478	71.6
HFV	1.60	117.4	2.880	1.400	117.4
HFV	1.60	117.4	3.000	1.363	139.1
$\Lambda_{\text{BroB}}^{\text{RBHF}}$ + HFV	1.62	127.5	2.473	$\cdots$	$\cdots$
$\Lambda_{\text{BroB}}^{\text{RBHF}}$ + HFV	1.62	127.5	2.600	1.50	69.6
$\Lambda_{\text{BroB}}^{\text{RBHF}}$ + HFV	1.62	127.5	2.880	1.41	121.7
$\Lambda_{\text{BroB}}^{\text{RBHF}}$ + HFV	1.62	127.5	3.000	1.38	139.1
$G_{\text{M78}}^{\text{K240}}$	1.56	96.3	2.473	1.48	48.2
$G_{\text{M78}}^{\text{K240}}$	1.56	96.3	2.600	1.45	66.2
$G_{\text{M78}}^{\text{K240}}$	1.56	96.3	2.880	1.37	114.4
$G_{\text{M78}}^{\text{K240}}$	1.56	96.3	3.000	1.33	138.4
$G_{\text{M78}}^{\text{K240}}$(NP)	1.56	96.3	2.473	1.48	48.2
$G_{\text{M78}}^{\text{K240}}$(NP)	1.56	96.3	2.600	1.45	66.2
$G_{\text{M78}}^{\text{K240}}$(NP)	1.56	96.3	2.880	1.37	114.4
$G_{\text{M78}}^{\text{K240}}$(NP)	1.56	96.3	3.000	1.33	138.4

FIG. 5. Effect of strange-quark mass, m_s, on the pressure P. P_0 is the zero quark mass pressure of strange-quark matter about the same energy density ϵ.

of the strange-quark mass on the strange star structure is small. The correction to the maximum mass of quark stars due to a quark mass up to 150 (225) MeV for each series of Λ is less than 3 (10)% (Table II). Since the experimental data show that the mass of a strange quark is ~150 MeV, we can safely ignore the quark mass when calculating the global properties of a quark star.

A recent study shows that quark matter in the color-flavor locked (CFL) phase can be electrically neutral, even though the quark masses are unequal. Electrons are not needed to maintain the charge neutrality [27]. However, the CFL phase occurs at the very high density regime. Electrons or positrons may still be present near the surface of a quark star, and they are important for its cooling behavior. More detailed discussion of the effect of massive strange quarks and its physical implications can be found in Refs. [25,26,28,29].

V. PHASE TRANSITION FROM STRANGE STARS TO NEUTRON STARS

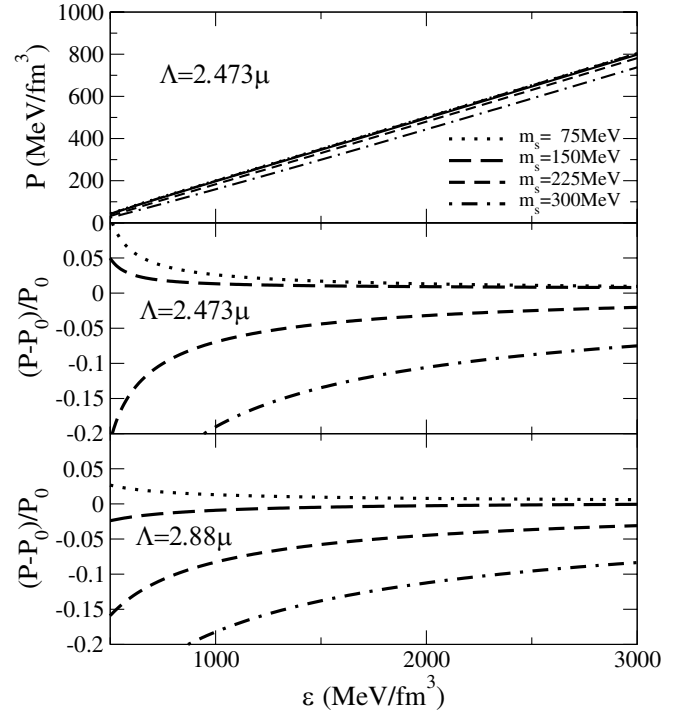It has long been suggested that strange stars can be formed from a phase transition of neutron stars to strange stars due to an abrupt increase in density [30,31]. However, from a theoretical point of view, formation of quark-gluon plasma is favored when both temperature and chemical potential are high enough [12]. Hence it is reasonable to suggest that strange stars are formed in supernovae where both high temperature and density

TABLE II. Effect of strange-quark mass on the global structure of a strange star. The superscripts of "max" correspond to quantities of maximum mass stars.

m_s (MeV)	$\epsilon_c^{\max}(\epsilon_0)$	$M^{\max}(M_\odot)$	% increase	$R^{\max}$ (km)	% increase
		$\Lambda = 2.473\mu$			
0	12.0	1.516	$\cdots$	8.54	$\cdots$
75	12.3	1.550	+2.22%	8.64	+1.17%
150	12.1	1.533	+1.11%	8.59	+0.59%
225	14.0	1.441	−4.95%	8.15	−4.57%
300	16.1	1.323	−12.75%	7.69	−9.95%
		$\Lambda = 2.88\mu$			
0	8.0	1.983	$\cdots$	11.07	$\cdots$
75	7.2	2.022	+1.93%	11.33	+2.35%
150	7.3	1.956	−1.36%	11.08	+0.09%
225	8.8	1.796	−9.46%	10.35	−6.50%
300	9.5	1.641	−17.26%	9.92	−10.39%

are achieved [13]. If the strange-quark matter is absolutely stable for high density and zero temperature, i.e., $\Lambda/\mu \gtrsim 2.88$, the quark star will remain in the quark phase even when it cools down. If the strange star is energetically less stable than a neutron star below some temperature, it will cool down to the phase transition temperature, T_p, and change into a neutron star containing ordinary baryons. If the baryonic mass M_B is conserved during the phase transition, the total conversion energy E_{conv} released is given by

$$E_{\text{conv}} = [M_G(\text{SS}) - M_G(\text{NS})]c^2, \quad (17)$$

where $M_G(\text{SS})$ and $M_G(\text{NS})$ are the gravitational masses of the strange star and neutron star, respectively [32]. Whether a phase transition can occur and how much energy is released depend on both the EOS's of quark matter and nuclear matter. We are interested in the possibility that strange-quark matter is only stable for $T > T_p$, and so we choose a $\Lambda/\mu < 2.7$, so that when the hot strange star cools to low temperature, it will convert to a neutron star. For $\Lambda/\mu = 2.473$, the maximum gravitational mass is $1.516 M_\odot$ with a baryonic mass of $1.60 M_\odot$ and radius 8.54 km. We will use this set of parameters in the calculation of the cooling behavior because the maximum mass is close to observational data of compact stars. In fact, we have used other values of Λ/μ, and the cooling behavior is qualitatively similar, as long as the star undergoes a phase transition. The cold EOS of the neutron stars will determine only the conversion energy. The cooling behavior is determined by the cooling mechanisms and heat capacities in our calculations. We simply choose the HFV EOS based on the relativistic Hartree-Fock approximation [24] to calculate the conversion energy. A typical neutron star with $M_B = 1.60 M_\odot$ and $M_G = 1.40 M_\odot$ is chosen [24] in the cooling calculations. For comparison, the energy released for different Λ/μ, together with several commonly used neutron star EOS's, is summarized in Table III. For $\Lambda/\mu = 2.473$, typically 10^{53} erg is released during the process, which depends only weakly on the nuclear matter EOS. We propose that it can be an energy source of GRB's [26].

VI. COOLING PROPERTIES

It is believed that in an ultrarelativistic heavy-ion collision, a hot quark-gluon plasma is formed initially, which then cools down to the phase transition temperature T_p and goes into the mixed phase, if the QCD phase transition is first order. When all the quark matter has hadronized, the temperature drops again [33]. We borrow this idea to describe the cooling of a strange star. When the strange star is born, the temperature can be as high as a few times 10^{11} K [34]. The surface is so hot that all the materials, other than strange-quark matter, are evaporated leaving the strange star nearly bare without any crust [10]. Since the thermal conductivity of strange-

TABLE III. Total conversion energy E_{conv} released of a compact star for different Λ. The neutron star gravitational mass $M_G = 1.4 M_\odot$ with various EOS's.

EOS (NS)	$M_B/M_\odot$	Λ/μ	$M_G(\text{SS})/M_\odot$	$E_{\text{conv}}/10^{53}$ erg
HV	1.51	2.473	1.44	+0.72
HV	1.51	2.600	1.41	+0.18
HV	1.51	2.880	1.33	−1.25
HV	1.51	3.000	1.29	−1.97
HFV	1.60	2.473	1.516	+2.08
HFV	1.60	2.600	1.478	+1.40
HFV	1.60	2.880	1.400	0
HFV	1.60	3.000	1.363	−0.66
$\Lambda_{\text{BroB}}^{\text{RBHF}}$ + HFV	1.62	2.473	$\cdots$	$\cdots$
$\Lambda_{\text{BroB}}^{\text{RBHF}}$ + HFV	1.62	2.600	1.50	+1.79
$\Lambda_{\text{BroB}}^{\text{RBHF}}$ + HFV	1.62	2.880	1.41	+0.18
$\Lambda_{\text{BroB}}^{\text{RBHF}}$ + HFV	1.62	3.000	1.38	−0.36
$G_{\text{M78}}^{\text{K240}}$	1.56	2.473	1.48	+1.43
$G_{\text{M78}}^{\text{K240}}$	1.56	2.600	1.45	+0.90
$G_{\text{M78}}^{\text{K240}}$	1.56	2.880	1.37	−0.54
$G_{\text{M78}}^{\text{K240}}$	1.56	3.000	1.33	−1.25
$G_{\text{M78}}^{\text{K240}}$(NP)	1.56	2.473	1.48	+1.43
$G_{\text{M78}}^{\text{K240}}$(NP)	1.56	2.600	1.45	+0.90
$G_{\text{M78}}^{\text{K240}}$(NP)	1.56	2.880	1.37	−0.54
$G_{\text{M78}}^{\text{K240}}$(NP)	1.56	3.000	1.33	−1.25

quark matter is very high and the density profile of the strange star is very flat, we will take the uniform temperature and density approximation. Hence the strange star cools down according to the equation:

$$C_q \frac{dT}{dt} = -L_q, \quad (18)$$

where C_q is the total heat capacity of all the species in quark matter, and L_q is the total luminosity of the star. When the temperature drops to T_p, the strange star undergoes a phase transition and a latent heat E_{conv} is released. We simply take T_p to be constant in density throughout the star, which has a much smaller value than the zero chemical potential value of about 150 MeV because of the high chemical potential. During the phase transition, we assume that the quark and neutron matter are distributed uniformly and calculate the luminosity of the mixed phase by the weighted average of that of the quark matter and the neutron matter (Sec. VI D). When the strange star has lost all its latent heat and converted completely to a neutron star, it then follows the standard cooling of a neutron star with an initial temperature of T_p. The detailed thermal evolution is governed by several energy transport equations. We adopt a simple model that a neutron star has a uniform temperature core with high conductivity and two layers of crust, the inner crust and the outer crust, which transport heat not as effectively as the core or quark matter. The typical thickness of the

crust is $\sim 10\%$ of the radius, and we can use the parallel-plane approximation to describe the thermal evolution of the inner crust. The thermal history of the inner crust can be described by a heat conduction equation:

$$c_{\mathrm{crust}}\frac{\partial T}{\partial t} = \frac{\partial}{\partial r}\left(K\frac{\partial T}{\partial r}\right) - \epsilon_\nu, \qquad (19)$$

where c_{crust} is the specific heat of the inner crust, K is the effective thermal conductivity, and ϵ_ν is the neutrino emissivity. As a rule of thumb, the effective surface temperature T_s and the temperature at the interface of the inner and outer crusts T_b are related by [35]

$$T_{b8} = 1.288(T_{s6}^4/g_{s14})^{0.455}, \qquad (20)$$

where g_{s14} is the surface gravity in the unit of $10^{14}\,\mathrm{cm\,s^{-2}}$, T_{b8} is the temperature between the inner and outer crusts in the unit of 10^8 K, and T_{s6} is the effective surface temperature in the unit of 10^6 K. The luminosity at the stellar surface, L_{surface}, is equal to the heat flux at the interface of the inner and the outer crusts:

$$-K\frac{\partial T}{\partial r} = L_{\mathrm{surface}}/(4\pi R^2), \qquad (21)$$

where R is the radius of the star. The boundary condition at the interface of the core and inner crust is

$$C_{\mathrm{core}}\frac{\partial T}{\partial t} = -K\frac{\partial T}{\partial r}A_{\mathrm{core}} - L_\nu^{\mathrm{core}}, \qquad (22)$$

where C_{core} is the total heat capacity of the core, A_{core} is the surface area of the core, and L_ν^{core} is the total neutrino luminosity of the core.

A. Heat capacity of quark stars

The total heat capacity is the sum of the heat capacities of all species in the star. Without the effect of superfluidity, the quark matter can be considered as a free Fermi gas, and the specific heat of quark matter is given by [36,37]

$$c_q = 2.5 \times 10^{20}(\rho/\rho_0)^{2/3}T_9\,\mathrm{erg\,cm^{-3}\,K^{-1}}, \qquad (23)$$

where ρ is the baryon density and $\rho_0 = 0.17\,\mathrm{fm^{-3}}$ is the nuclear matter density. Some authors may use energy density instead of number density. The difference is only of a numerical factor and does not change the cooling curve much. In the superfluid state, the quarks will form Cooper pairs. The specific heat will be modified as [38,39]

$$c_q^{\mathrm{sf}} = \begin{cases} \frac{3.15c_q}{\tilde{T}}e^{-1.76/\tilde{T}}[2.5 - 1.66\tilde{T} + 3.64\tilde{T}^2] & \text{for } 0.2 \le \tilde{T} \le 1, \\ 0 & \text{for } \tilde{T} < 0.2, \end{cases} \qquad (24)$$

where $k_B T_c = \Delta/1.76$, $\tilde{T} = T/T_c$, and Δ is the energy gap in MeV in BCS theory. It has been argued that for quark matter, even with unequal quark masses, in the CFL phase in which all three flavors and colors are paired, quark matter is automatically charge neutral and no electrons are required [27]. However, for sufficiently large strange-quark mass and the relatively low density regime near the stellar surface, the two color-flavor superconductor phase is expected to be preferred. Therefore in a real strange star, electrons are believed to be present. The contribution of electrons can be parametrized by the electron fraction Y_e, which depends on the model of strange stars. We choose $Y_e = 0.001$ as a typical value. The specific heat capacity of electrons in the strange star phase is given by [8]

$$c_e = 1.7 \times 10^{20}\left(\frac{Y_e\rho}{\rho_0}\right)^{2/3}T_9\,\mathrm{erg\,cm^{-3}\,K^{-1}}. \qquad (25)$$

The heat capacity of electrons is unaffected by the superfluidity of quark matter. Hence it dominates the total heat capacity of the strange star when the temperature drops below T_c.

B. Luminosity of quark stars

The total luminosity is the sum of contributions from all energy emission mechanisms, including both photon and neutrino emissions. The cooling of quark-gluon plasma has been studied for many years [24] and can be divided into fast and slow cooling processes. Two of the most popular fast cooling processes are the electron-positron pair production and quark URCA process. Two well-known slow cooling processes are thermal equilibrium and nonequilibrium blackbody radiation. We have included all these cooling processes in our calculations. The recently proposed pion production in a strange star is found to be a very effective cooling mechanism, and it may explain the energy supply of GRB's [8]. Therefore we also studied the effect of the pion production cooling. Luminosities of various cooling mechanisms are plotted in Figs. 6 and 7.

1. Pion production

It is known that for a hot quark-gluon plasma described by a cloudy bag model, pions can be produced through two mechanisms: thermal excitation and collisions between quarks and the bag surface [8,40,41]. When the pions leave the quark star surface, they will decay into photons and e^+e^- pairs through the following channels:

$$\pi^0 \rightarrow 2\gamma \leftrightarrow e^+e^-, \qquad (26)$$

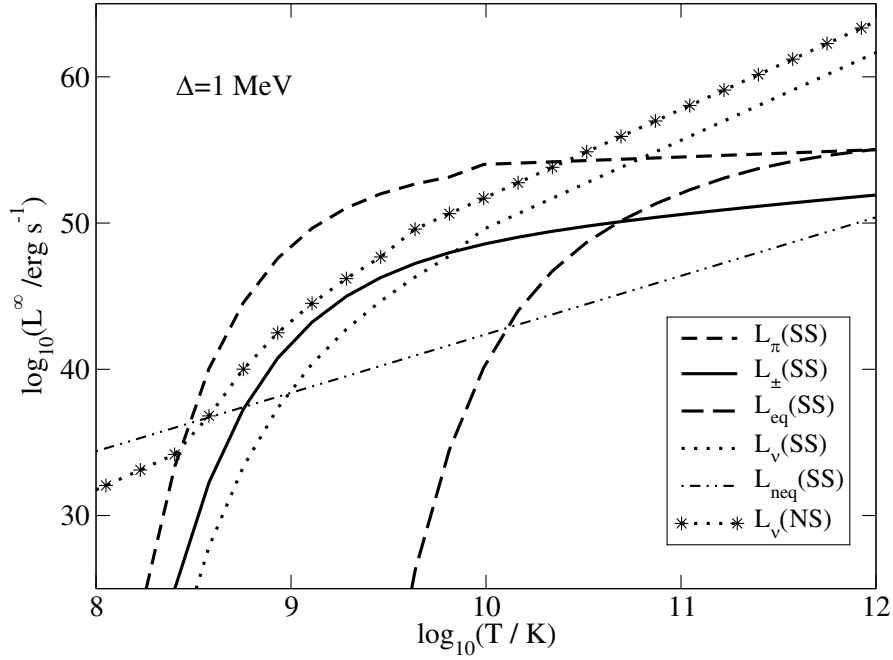$$\pi^\pm \rightarrow \mu^\pm + \nu_\mu, \qquad (27)$$

FIG. 6. Observed luminosity L^∞ as a function of temperature T for a small superfluid gap model in the quark phase $\Delta = 1$ MeV. L_π, $L_\pm$, L_{eq}, L_ν, and L_{neq} denote the pion, e^+e^-, thermal equilibrium radiation, neutrino emission, and nonequilibrium blackbody radiation luminosity, respectively. For comparison, the neutrino luminosity of the neutron star phase is also plotted. SS and NS correspond to strange stars and neutron stars, respectively [8].

$$\mu^\pm \rightarrow e^\pm + \nu_e + \nu_\mu. \qquad (28)$$

It has been shown that the production of pions is a very powerful source of e^+e^- pairs and photons, with luminosity $\sim 10^{54}$ erg s^{-1}. Such a powerful source of e^+e^-

pairs and photons may serve as the source engine of γ-ray bursts. The pion emissivity is estimated to be [8]

$$L_\pi = \rho_\pi \sqrt{\frac{2k_B T}{m_\pi}} 4\pi R^2, \qquad (29)$$
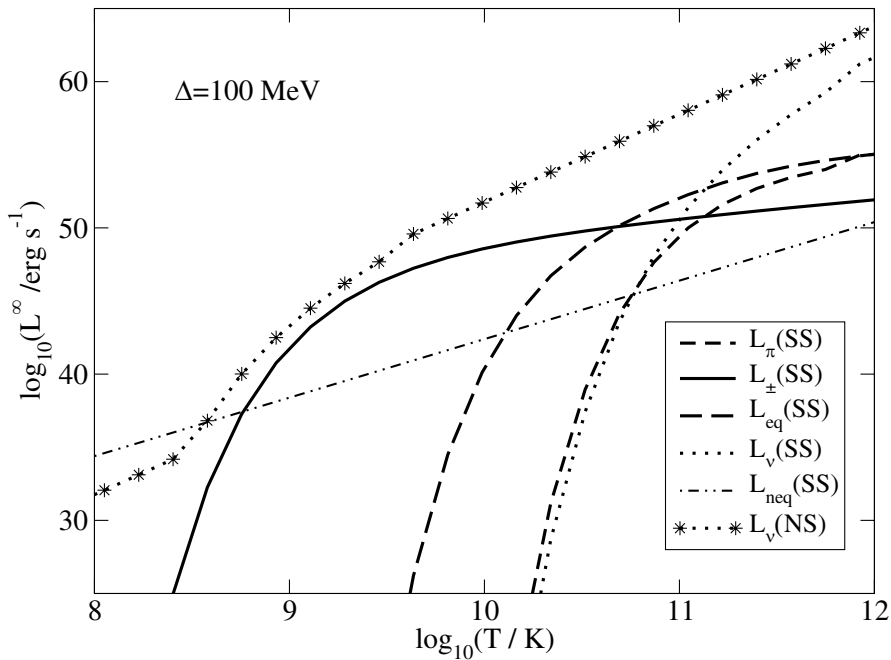

FIG. 7. Same as Fig. 6, but for a large superfluid gap model in the quark phase $\Delta = 100$ MeV [8].

where $\rho_\pi = 7.1 \times 10^{31}$ erg cm^{-3} is the energy density of the pion field at the stellar surface, T is the temperature of the quark star, which is taken to be uniform, and $m_\pi = 140$ MeV is the pion mass. In the superfluid state, the collisions between quarks are suppressed due to the pair up of quarks, and the pion luminosity is then reduced by a factor of $\exp(-\Delta/T)$.

2. Quark URCA process

The dominating neutrino emission process is the quark URCA process:

$$d \rightarrow u + e + \overline{\nu}_e, \tag{30}$$

$$u + e \rightarrow d + \nu_e. \tag{31}$$

The neutrino emissivity was estimated as [36]

$$\epsilon_d \simeq 2.2 \times 10^{26} \alpha_s \left(\frac{\rho}{\rho_0}\right) Y_e^{1/3} T_9^6 \text{ erg cm}^{-3}\text{ s}^{-1}, \tag{32}$$

where α_s is the strong coupling constant, and we have chosen $\alpha_s = 0.4$ as a constant value throughout the quark star. Note that the definition of the strong coupling constant is different from that of Iwamoto's. In the superfluid state, the neutrino emissivity is suppressed by a factor of $\exp(-\Delta/T)$.

3. Electron-positron pair production

It has been pointed out that the bare surface of a hot strange star is a powerful source of e^+e^- pairs due to the strong electric field at the surface [9]. The e^+e^- pair production rate is [10]

$$\dot{n}_\pm \simeq 10^{39} T_9^3 \exp(-11.9/T_9) J(\xi) \text{ s}^{-1}, \tag{33}$$

where

$$J(\xi) = \frac{1}{3} \frac{\xi^3 \ln(1 + 2\xi^{-1})}{(1 + 0.074\xi)^3} + \frac{\pi^5}{6} \frac{\xi^4}{(13.9 + \xi)^4}, \tag{34}$$

$$\xi = 2\sqrt{\frac{\alpha}{\pi}} \frac{\varepsilon_F}{k_B T} \simeq 0.1 \frac{\varepsilon}{k_B T}, \tag{35}$$

$\alpha = 1/137$ is the fine-structure constant and $\varepsilon_F = 18$ MeV is the Fermi energy of electrons. The luminosity of e^+e^- pairs is given by

$$F_\pm \simeq \varepsilon_\pm \dot{n}_\pm, \tag{36}$$

where $\varepsilon_\pm \simeq m_e c^2 + k_B T$ is the mean energy of created particles.

4. Thermal equilibrium radiation

The thermal equilibrium radiation of frequency ω less than the plasma frequency $\omega_p \simeq 20\text{–}25$ MeV is greatly suppressed due to the very high density of the quark-gluon plasma [6,10]. The luminosity of thermal equilib-

rium photons is [10]

$$F_{\text{eq}} = \int_{\omega_p}^{\infty} d\omega \frac{\omega(\omega^2 - \omega_p^2)g(\omega)}{\exp(\omega/T) - 1}, \tag{37}$$

where

$$g(\omega) = \frac{1}{2\pi} \int_0^{\pi/2} d\theta \sin\theta \cos\theta D(\omega, \theta), \tag{38}$$

$D(\omega, \theta) = 1 - (R_\perp + R_\parallel)$ is the coefficient of radiation transmission from the quark-gluon plasma to vacuum, with

$$R_\perp = \frac{\sin^2(\theta - \theta_0)}{\sin^2(\theta + \theta_0)}, \qquad R_\parallel = \frac{\tan^2(\theta - \theta_0)}{\tan^2(\theta + \theta_0)}, \tag{39}$$

$$\theta_0 \equiv \arcsin[\sin\theta\sqrt{1 - (\omega_p/\omega)^2}]. \tag{40}$$

5. Nonequilibrium blackbody radiation

The above processes are very powerful sources of energy emission and will dominate the cooling process at very high temperature. Once the temperature drops, the cooling process will be dominated by the relatively low power nonequilibrium blackbody radiation [42]:

$$L_{\text{neq}} \approx 10^{-6} L_{\text{bb}}, \tag{41}$$

where $L_{\text{bb}} = 4\pi R^2 \sigma T^4$ is the blackbody radiation luminosity.

C. Microphysics of the neutron star cooling

There are many different models of neutron star cooling. Since we mainly focus on the cooling of the quark phase and examine the phase transition process qualitatively, the cooling of neutron stars can be taken from any model available in the literature. We simply adopt the model of neutron stars described by Ng et al. [8,39]. The heat capacities of neutron matter in both normal and superfluid states and of the electrons are

$$c_n = 2.3 \times 10^{39} M_* \rho_{14}^{-2/3} T_9 \text{ erg K}^{-1}, \quad \text{for } \tilde{T} > 1, \tag{42}$$

$$c_n^{\text{sf}} = \frac{3.15 c_n}{\tilde{T}} e^{-1.76/\tilde{T}}[2.5 - 1.66\tilde{T} + 3.64\tilde{T}^2], \\ \text{for } 0.2 \leq \tilde{T} \leq 1, \tag{43}$$

and

$$c_e = 1.9 \times 10^{37} M_* \rho_{14}^{1/3} T_9 \text{ erg K}^{-1}, \tag{44}$$

where M_* is the mass of the neutron star in units of solar mass, $\rho_{14} = \rho/10^{14}$ g cm^{-3}, and we take $T_c = 3.2 \times 10^9$ K for our calculations.

The neutrino emission mechanisms are the direct URCA process:

$$n \rightarrow p + e^- + \overline{\nu}_e, \tag{45}$$

$$p + e^- \rightarrow n + \nu_e, \tag{46}$$

with the neutrino emissivity [8,43]:

$$\epsilon_{\mathrm{URCA}} = 4.00 \times 10^{27} (Y_e \rho / \rho_0)^{1/3} T_9^6 \ \mathrm{erg\,cm^{-3}\,s^{-1}}, \\ \text{for } T > T_c, \tag{47}$$

$$\epsilon_{\mathrm{URCA}}^{\mathrm{sf}} = \epsilon_{\mathrm{URCA}} \exp(-\Delta/T), \quad \text{for } T < T_c, \tag{48}$$

with $Y_e = 0.1$, electron-proton Coulomb scattering in the crust:

$$e + p \rightarrow e + p + \nu + \overline{\nu} \tag{49}$$

with luminosity [8,44]:

$$L_\nu^{\mathrm{cr}} = 1.7 \times 10^{39} M_* (M_{\mathrm{cr}}/M) T_9^6 \ \mathrm{erg\,s^{-1}}, \tag{50}$$

where (M_{cr}/M) is the fractional mass of the crust $\approx 5\%$, and the neutrino bremsstrahlung process:

$$n + n \rightarrow n + n + \nu + \overline{\nu} \tag{51}$$

with luminosity [8]:

$$L_\nu^{\mathrm{nn}} = 4.3 \times 10^{38} \rho_{14}^{1/3} T_9^8 \ \mathrm{erg\,s^{-1}}, \quad \text{for } T > T_c, \\ = 0 \qquad\qquad\qquad\qquad \text{for } T \leq T_c. \tag{52}$$

The surface luminosity will be of the blackbody radiation with the effective surface temperature T_s:

$$L_{\mathrm{bb}} = 4\pi R^2 \sigma T_s^4. \tag{53}$$

The blackbody radiation will be the dominating cooling mechanism after the neutrino emission processes are switched off.

For the thermal conductivity of the inner crust, we simply choose a temperature dependent model [45]:

$$K = \frac{2.8 \times 10^{20}}{T_{10}} \ \mathrm{erg\,cm^{-1}\,s^{-1}\,K^{-1}}. \tag{54}$$

The choice of thermal conductivity will not be important after the epoch of thermal relaxation, which is of the order 10–100 years. The temperature of the inner crust and the core will be uniform after that.

D. Handling of the phase transition

The actual situation during the phase transition is very complicated, involving detailed hydrodynamical simulations, how quark matter is transformed into ordinary hadronic matter, and so on. Many authors have discussed the theoretical modeling of the phase transition in heavy-ion collisions, neutron star-strange star phase transition, and the cosmological quark-hadron transition, but the uncertainties are of course very large at this stage. Without involving the details, we simply assume that the phase transition is first order and evolves quasistatically. The quark and neutron matter are distributed uniformly in the mixed phase. We develop a simple model to describe the luminosities of the mixed phase in order to capture the main features just before and after the phase transition. The detailed results during the phase transition are of course inaccurate, but the main features should be approximately correct, as long as the phase transition does not disrupt the neutron star completely.

The energy loss during the phase transition is

$$E_{\mathrm{loss}} = \int_{t_0^{\mathrm{PT}}}^t L_q^{\mathrm{PT}} + L_n^{\mathrm{PT}} dt, \tag{55}$$

where L_q^{PT} and L_n^{PT} are the total luminosity of the quark matter contribution and nuclear matter contribution during the phase transition, respectively, and t_0^{PT} is the starting time of the phase transition. We define the fractions of the total baryonic number of quarks and neutrons in the mixed phase to be A_{SS} and A_{NS}, respectively. A_{SS} and A_{NS} will be related to the conversion energy E_{conv} and energy loss during the phase transition E_{loss} by

$$A_{\mathrm{SS}} = \frac{E_{\mathrm{conv}} - E_{\mathrm{loss}}}{E_{\mathrm{conv}}} \tag{56}$$

and

$$A_{\mathrm{NS}} = \frac{E_{\mathrm{loss}}}{E_{\mathrm{conv}}}. \tag{57}$$

1. Pion production, $e^+ e^-$ pair production

Since the pion production and $e^+ e^-$ pair production are the features of a hot quark star, we expect the production rates to decrease with the fraction of quark number during the phase transition. We simply treat the luminosities of both contributions to be

$$L_{\pi(e^+ e^-)}^{\mathrm{PT}} = A_{\mathrm{SS}} L_{\pi(e^+ e^-)}. \tag{58}$$

2. Thermal equilibrium radiation

The plasma frequency is related to the baryon number density as [10]

$$\omega_p = \left(\frac{8\pi}{3} \frac{e^2 c^2 n_b^2}{\mu}\right)^{1/2}, \tag{59}$$

where $\mu \simeq \hbar c (\pi^2 n_b)^{1/3}$ is the chemical potential. Hence,

$$\omega_p \propto n_b^{1/3}. \tag{60}$$

For a typical strange star, $\omega_p \simeq 20$ MeV. Therefore during the phase transition, the plasma frequency will be related to the fraction of quark number as

$$\omega_p^{\mathrm{PT}} \simeq 20 A_{\mathrm{SS}}^{1/3} \ \mathrm{MeV}. \tag{61}$$

The luminosity of thermal equilibrium photons during the phase transition is given by Eq. (37) where $\omega_p = \omega_p^{\mathrm{PT}}$. We can see that the lower limit becomes smaller during the phase transition. The luminosity reduces to that of thermal blackbody radiation at the end of the phase

transition. Hence we expect an increase of equilibrium photon luminosity as a signature of the phase transition.

3. Quark URCA process

From Eq. (32), the neutrino emissivity of a quark star $\epsilon_d \propto \rho$. Hence,

$$\epsilon_d^{\mathrm{PT}} = \epsilon_d A_{\mathrm{SS}}. \tag{62}$$

4. Neutrino emission process of the neutron matter

For the neutrino emissivity of neutron matter, we use the fractional density of neutron matter in the density dependent terms of Eqs. (47) and (52), i.e.,

$$\rho \rightarrow A_{\mathrm{NS}}\rho. \tag{63}$$

For the electron-proton Coulomb scattering of Eq. (50), we simply calculate its contribution with a weighted mean:

$$L_\nu^{\mathrm{crPT}} = L_\nu^{\mathrm{cr}} A_{\mathrm{NS}}. \tag{64}$$

Lattimer *et al.* pointed out that a direct URCA process can only be switched on in a neutron star at sufficiently high central density [43]. For a wide range of parameters, the required central density is of the order of nuclear matter density. We switch on the direct URCA process only when the average density of neutron matter is above the nuclear matter density.

5. Nonequilibrium blackbody radiation

Since the nonequilibrium blackbody radiation is not the dominating cooling mechanism in the temperature range of 10^9–10^{11} K, it can be neglected in the mixed phase.

VII. THE MODELS

When a strange star is born just after the stellar collapse, its temperature is very high $\sim 10^{11}$ K ~ 40 MeV [14]. We choose an initial temperature $T_i = 40$ MeV. The EOS of perturbative QCD with massless quarks and temperature correction up to first order in α_s is [46]

$$P = \frac{8\pi^2}{45}T^4\left(1 - \frac{15}{4}\frac{\alpha_s}{\pi}\right) + \sum\left[\frac{7}{60}\pi^2 T^4\left(1 - \frac{50}{21}\frac{\alpha_s}{\pi}\right)\right.$$
$$\left. + \left(\frac{1}{2}T^2\mu_f^2 + \frac{1}{4\pi}\mu_f^4\right)\left(1 - 2\frac{\alpha_s}{\pi}\right)\right]. \tag{65}$$

Since just after the collapse, $T \sim 40$ MeV $\ll \mu \sim 300$ MeV at the surface, the zero temperature EOS is appropriate for calculating the structure of the star. In our cooling model, the only free parameter of the EOS in the quark phase is Λ. It will determine whether a phase transition can occur and how much latent heat can be released. For a $1.4M_\odot$ compact star, the cooling curves are mainly affected by the cooling mechanisms and heat

TABLE IV. Models of quark phase presented in this paper.

| | Cooling mechanisms | | | | | Superfluid gap |
Model	Quark URCA	neq	eq	e^+e^-	Pion	Δ (MeV)
(a)	$\checkmark$	$\checkmark$	$\checkmark$	$\times$	$\checkmark$	1
(b)	$\checkmark$	$\checkmark$	$\checkmark$	$\checkmark$	$\checkmark$	1
(c)	$\checkmark$	$\checkmark$	$\checkmark$	$\checkmark$	$\times$	1
(d)	$\checkmark$	$\checkmark$	$\checkmark$	$\checkmark$	$\times$	100
(e)	$\checkmark$	$\checkmark$	$\checkmark$	$\checkmark$	$\checkmark$	100
(f)	$\checkmark$	$\checkmark$	$\checkmark$	$\times$	$\checkmark$	100

capacities of the material, rather than Λ, which mainly affects the structure of the compact star. Therefore we choose only one value of this parameter, $\Lambda = 2.473\mu$, for the cooling calculations. The phase transition temperature T_p involves detailed study of the baryon phase diagram, which is still highly uncertain. The latest results [15,16] indicate that T_p drops from its zero density value of 140 MeV to a few MeV for a density of a few times nuclear matter density. Hence we treat T_p as a parameter and study the cooling behaviors for different T_p. We assume a constant T_p in density throughout the star and present results for $T_p = 1$, 10 MeV for comparison. The remaining ingredients are the heat capacities and cooling mechanisms of the star. For the quark phase, the URCA process, thermal equilibrium and nonequilibrium radiation are believed to occur for a bare strange star. We include all these processes in our calculations, and we choose other combinations of cooling processes to investigate the effect of each cooling mechanism. For the superfluid phase of quark matter, we choose $\Delta = 1$ MeV for a small gap model and $\Delta = 100$ MeV for a large gap model. The various models presented in this paper are summarized in Table IV.

VIII. RESULTS

The strange star luminosity L discussed above is typically many orders of magnitude higher than 10^{37} erg/s and may be as high as 10^{53} erg/s. In this case, the outflowing wind is optically thick, and at $L > 10^{42}$–10^{43} erg/s the spectrum of emergent photons is nearly a blackbody spectrum [47,48]. Therefore, for a newborn strange star, the pion production, equilibrium radiation, and electron-positron pair production cannot be distinguished observationally in spite of the fact that the characteristic gamma-ray energies at these processes near the strange star surface differ significantly. They can be distinguished observationally only if the phase transition temperature is very low, such that the strange star can exist in a relatively low temperature. The observables are the luminosity and the surface temperature at infinity, L^∞ and T_s^∞, which are related to the stellar surface values, L and T_s [49]:

$$T_s^\infty = e^{\phi_s} T_s, \qquad (66)$$

$$L^\infty = e^{2\phi_s} L, \qquad (67)$$

where $e^{\phi_s} = \sqrt{1 - 2M/R}$ is the gravitational redshift at the stellar surface. The various cooling curves for different models are shown in Figs. 8(i)–(iv). Models (a)–(c) are small superfluid gap models, while models (d)–(f) are large superfluid gap models. For small (large) superfluidity gap models, the phase transition temperature considered here is well above (below) the superfluid gap. We can get some insight of the effect of superfluidity on the signatures of phase transition.

A. Models (a), (b)

The cooling curves for model (a) and model (b) are nearly the same. It is because both of them have the same thermal properties, and all the cooling mechanisms are switched on, except for model (a) that the $e^- e^+$ pair production is not considered. Since for the small superfluid gap $\Delta = 1$ MeV, pion emission is not suppressed for $T > T_c$. The pion emissivity dominates the $e^- e^+$ pair production by several orders of magnitude at high temperature. At low temperature, the cooling process will be dominated by the blackbody radiation. Hence both models will be dominantly cooled by the same mechanisms and have the same cooling history. Only if the phase
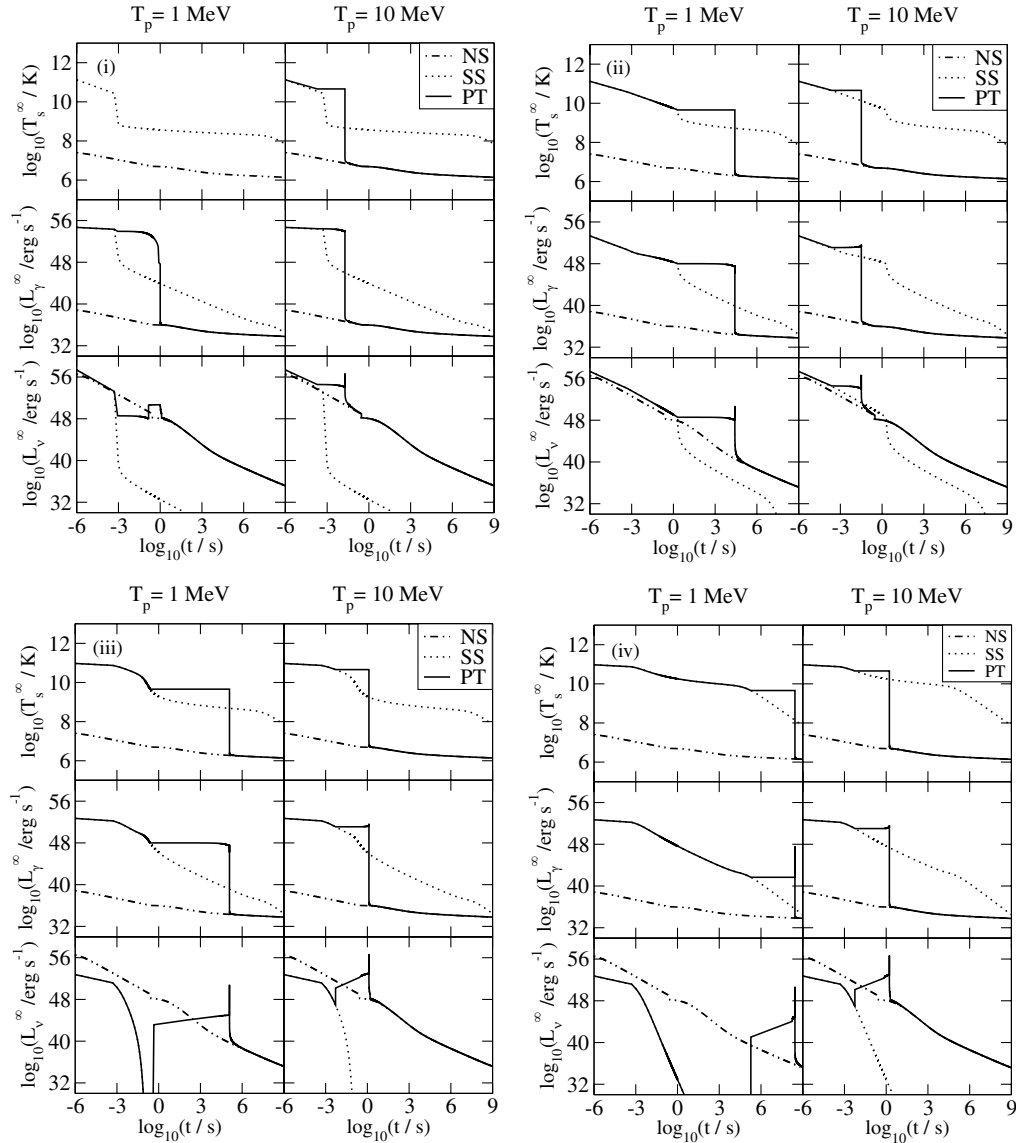

FIG. 8. Cooling curves corresponding to different models. (i) corresponds to models (a) and (b). (ii) corresponds to model (c). (iii) corresponds to models (d) and (e). (iv) corresponds to model (f). In each figure, the left (right) panels are for models with small (large) phase transition temperature $T_p = 1$ (10) MeV. The dotted (dashed) lines are the cooling curves of a pure strange (neutron) star without phase transition. The solid line represents the scenario with phase transition. T_s^∞, L_γ^∞, and L_ν^∞ denote surface temperature, photon luminosity, and neutrino luminosity, respectively. An initial temperature of 40 MeV is assumed.

transition temperature is very low, can we distinguish them by studying the spectrum, in which model (b) shows the character of $e^- e^+$ production. In these models, for $T_p = 1$ MeV, the photon luminosity can maintain up to 10^{50}–10^{54} erg s^{-1} for about 1 s when the star is in the quark and mixed phases. Such a "long" duration of extremely high luminosity, compared to Ng *et al.*'s model which gives a luminosity that drops below 10^{50} erg s^{-1} within 0.01 s in the extreme case, is dominated by pion emission and maintained by the latent heat of the star. This violent fireball easily supplies the energy required for GRB's. The neutrino luminosity drops from 10^{57} to 10^{48} erg s^{-1} within 0.001 s and then rises to 10^{51} erg s^{-1} during the mixed phase which lasts for ~ 1 s.

This scenario of a second burst of neutrinos can be compared to two previous similar proposals [17,20]. In our model, the burst is due to the phase transition from a quark star to a neutron star, which has a higher neutrino emissivity, whereas in previous proposals, the second burst accompanies the phase transition from a neutron star to a quark star. In Benvenuto's theory, the phase transition is delayed by a few seconds after the core bounce due to the presence of the neutrinos [17]. In Aguilera *et al.*'s theory [20], the burst is due to the initial trapping of neutrinos when the temperature is high and their sudden release when the quark star cools. If quark matter is not as stable as nuclear matter at low temperature, then there should be yet another phase transition back to nuclear matter, which is what we focus on, and the "second" neutrino burst we propose is then the "third" neutrino burst.

If multiple neutrino bursts are observed, as may indeed be the case for the Kamiokande data for SN1987A [50], whether the compact star changes from the quark phase to the neutron phase (our model) or the other way around can be distinguished observationally in at least two ways. First, our model predicts that the cooling is much faster *before* the phase transition, but it will become slower *after* it. Second, the size of the post-phase-transition compact star, being a normal neutron star, would be larger in our model.

For $T_p = 10$ MeV, the high photon luminosity can be maintained only for ~ 0.02 s, since the neutrino luminosity is very high during the phase transition, in which it releases the latent heat within a short time. The rises in neutrino flux are about 2 orders of magnitudes, but the time scale is so short that they are likely to be masked by the diffusion time of neutrinos ($\sim 1 - 10$ s) [14] out of the dense medium and therefore probably indistinguishable from the first burst.

We have also studied the case of $T_p = 0.1$ MeV (not shown in the figures). The photon luminosity can be maintained at 10^{45} erg s^{-1} up to 5×10^6 s, and it then decreases gradually to 10^{34} erg s^{-1} in 10^{8-9} s, while the neutrino luminosity first drops to 10^{34} erg s^{-1} and then

rises to 10^{41} erg s^{-1} during the mixed phase. If such a long duration γ-ray source exists, it will be difficult to be explained by other models. For our model with $T_p \lesssim 0.01$ MeV (not shown), the cooling history is similar, but with an even longer duration and lower luminosities in the mixed phase.

The cooling curves (of all our models) are basically cooling of a bare quark star plus that of a neutron star. When the quark star cools to the phase transition temperature, the cooling curve switches from that of the quark star to the neutron star, plus a phase transition epoch. We can see that for a typical bare quark star without phase transition, the photon luminosity, as well as the surface temperature, is higher than that of the neutron star in the early epoch. The quark star then cools much faster than the neutron star, and it will be too cold to be observed. For the cooling of a bare quark star with phase transition, there is a significant feature different from the case without phase transition. When the quark star cools to the phase transition temperature, it remains at the phase transition temperature, and it releases the latent heat for a long time depending on the latent heat and the total luminosity. The total luminosity actually depends on the temperature. This means that the higher the phase transition temperature, the larger the luminosity and hence the shorter the duration of the phase transition. The latent heat depends on the choice of the EOS's of both the quark and the neutron matter, as well as the mass of the compact star. Here we have chosen $\Lambda = 2.473\mu$ for quark matter, the HFV EOS for neutron matter and a compact star mass of $\sim 1.4 M_\odot$. The latent heat is hence 2.08×10^{53} erg.

B. Model (c)

For model (c), the thermal properties are the same as models (a) and (b). In this model, the pion emissivity is not considered, and the dominating cooling process in the early epoch is the $e^- e^+$ production. Hence the photon luminosities for model (c) in the early epoch is significantly lower, and the durations of phase transition for high T_p models are longer. For $T_p = 1$ MeV, the photon luminosity drops from 10^{53} to 10^{48} erg s^{-1} and can maintain such a high luminosity up to 10^4 s. Such a model seems to be in good agreement with long duration GRB's both in the energy and time scales. For $T_p = 10$ MeV, the cooling curves are similar to those of models (a) and (b), except for the lower photon luminosity with a slight rise near the end of the phase transition in model (c). The similarity in cooling curves is due to the same dominating cooling mechanism of neutrino emission at the high temperature epoch in the quark and mixed phases, as well as the same cooling behavior after the phase transition. We have again studied the case for $T_p = 0.1$ MeV (not shown in the figure), the photon luminosity can be maintained up to 10^{38-39} erg s^{-1} for 10^{13-14} s. This model is

similar to Page and Usov's work [11], but our work can maintain a high luminosity for a much longer time. The late and phase transition epochs of the cooling curve for $T_p \lesssim 0.01$ MeV (not shown in the figure) are the same as those of models (a) and (b) at the same T_p. It is because for temperature $\lesssim 0.01$ MeV, the dominating cooling mechanisms in all models [including models (d) and (e) as well] in the quark and mixed phases are nonequilibrium blackbody radiation.

C. Models (d), (e)

As compared to models (a) and (b), the cooling curves for models (d) and (e) are also nearly identical. It is because the main effect of a large superfluid gap is to suppress pion and neutrino emissivities, which are important for the high temperature epoch. Hence the e^-e^+ production dominates the photon luminosity in the early epoch. Thus both models are dominantly cooled by the same mechanisms. We can see that the effect of superfluidity is to make the neutrino bursts more distinct. For $T_p = 10$ MeV, the neutrino flux rises by over 10 orders of magnitude within a small fraction of second. The effect may again be masked by the diffusion of neutrinos. However, if T_p is as low as 1 MeV, the two bursts of similar flux can be separated by as long as 10^5 s, which should be observable by modern neutrino observatories.

D. Model (f)

In model (f), e^-e^+ production is not considered. Although pion emissivity is included, it is again greatly suppressed. Hence the cooling history is as if there is no fast cooling mechanism. The quark star cools slowly, maintaining a relatively low photon luminosity for $\sim 10^8$ s for $T_p = 1$ MeV. One special feature of this model is that the photon luminosity rises up for about 6 orders of magnitude at the end of the phase transition for $T_p = 1$ MeV. This is due to the increase in luminosity of thermal equilibrium radiation during the phase transition (Sec. VI D). Indeed for models (a)–(e), if we separate the spectrum of thermal equilibrium radiation from other photon luminosities, it is also increasing. In our models, we expect more photons to be released during the phase transition. The duration is ~ 10 s in this model and shorter for other models. If such a burst is observed, it will be a unique feature which is difficult to be explained by other models. We remark here that detailed radiative transfer calculation may kill or lower the peak of this burst due to the surface effect of the star. Another special feature of this model is that for all models (a)–(e) [except model (c)], the second neutrino burst starts within 1 s from the first burst, which may be too short to be detected. This agrees with the observational data of SN1987a [14] (we emphasis here that based on the one event and the very few neutrinos detected, we really cannot tell how many neutrino bursts are there). In model (f), the second neutrino burst starts after 10^{4-5} s. Such a delayed neutrino burst may be detectable, and it may have significant effects on the propagation of shock waves in supernova remnants [14].

Remarks

In these models, we can see that the size of the superfluid gap determines how a compact star cools in the early epoch. Pion emission is a very efficient cooling mechanism if the superfluid gap is small. If the superfluid gap is large, e^-e^+ production will dominate in the early epoch. Also we find that a second neutrino burst is a signature of the phase transition, if the neutrino emissivity in the neutron phase is higher than that of the quark phase. In our models, the URCA process in a neutron star makes the second neutrino burst possible.

IX. DISCUSSION AND CONCLUSION

We studied the global structure and stability of strange stars with the perturbative QCD EOS up to order α_s^2. We find that for $\Lambda \gtrsim 2.88\mu$, strange-quark matter is absolutely stable, while for $\Lambda \gtrsim 2.35 \, (\gtrsim 2.7)\mu$, a strange star is globally stable (compared to a neutron star). The effect of strange-quark mass to the strange star is also studied. For a strange-quark mass $\lesssim 150 \, (225)$ MeV, the correction to the maximum mass of strange stars is less than 3 (10)%. We suggest that a strange star may undergo a phase transition to a neutron star when it cools down to some temperature T_p.

It has been argued that the rapid cooling of strange stars by pion emission can be a power source of GRB [8]. However, if the phase transition is not considered, the duration of the burst is too short, $<10^{-2}$ s, which cannot explain long duration GRB's, due to the rapid cooling without the maintenance of high temperature. However, in our model, the latent heat of the phase transition can supply the energy of the order 10^{53} erg. In our models, the photon luminosities can be maintained in 10^{48}–10^{54} erg s^{-1} with duration from $\sim 10^{-3}$ up to 10^4 s (or even longer), which are in the range for both long and short γ-ray bursts. Thus the latent heat solves the problem of the energy supply for the GRB's.

Another signature for quark stars that has been discussed is the relatively low luminosity of γ rays when the quark star cools down [11]. For models with low T_p, e.g., model (c) with $T_p \sim 0.1$ MeV, the luminosity due to the e^-e^+ pairs in the γ-ray range can be as high as 10^{38-39} erg s^{-1} with a very long duration of $\sim 10^{13-14}$ s, which is much longer than the case considered by Page and Usov [11]. The satellite Integral launched recently is sensitive just to γ rays in the energy range of 15 keV– 10 MeV. If a long duration γ-ray source is really detected, it would be a signature of the phase transition. On the

other hand, if no such source is detected, this does not mean failure of our models. Perhaps the phase transition temperature is very high, or the latent heat is small. Indeed Integral has already discovered a number of soft γ-ray point sources in the center of our galaxy [18]. Oaknin and Zhitnitsky have also discussed the possibility of the γ-ray sources being supermassive very dense droplets (strangelets) of dark matter in a recent paper [19].

If a second neutrino burst after a supernova explosion is detected, it will be strong evidence for the existence of a quark star, and in addition, it will support the switch on of the URCA process, or other fast neutrino emitting processes in neutron stars. However, the absence of the second burst does not kill quark stars, because there could simply be no fast neutrino emitting process in the neutron star phase, or the second burst arises so quickly that we cannot distinguish it from the first one.

It is generally believed that GRB's are related to supernovae [51–53]. Our model is compatible to the supernova connection—a supernova explosion leaves behind a compact star, which triggers the GRB weeks to years later. We suggest that the phase transition from a hot strange star to a neutron star may be the central engine of GRB's. During the phase transition, the size of the compact star increases, and an internal shock may develop, which initiates the GRB.

In our models, the phase transition is treated in an oversimplified manner. A detailed study should be made which involves hydrodynamics, the EOS, the emission properties of matter in the mixed phase, and so on. Also the duration of the quark phase may be so short that for the cooling process, the hydrostatic treatment of quark stars may not be appropriate. Hydrodynamic simulation may be needed for the whole process starting from the supernova explosion. This involves detailed numerical treatment which is beyond the scope of this paper. Here we discuss semiquantitatively the signatures left during the phase transitions by the presence of the quark phase, if it is reached in supernovae.

ACKNOWLEDGMENTS

[1] E. Witten, Phys. Rev. D **30**, 272 (1984).

[2] P. Slane, D. J. Helfand, and S. S. Murray, Astrophys. J. **571**, L45 (2002).

[3] S. Tsuruta et al., Astrophys. J. **571**, L143 (2002).

[4] J. J. Drake, H. L. Marshall, S. Dreizler, P. E. Freeman, A. Fruscione, M. Juda, V. Kashyap, F. Nicastro, D. O. Pease, B. J. Wargelin, and K. Werner, Astrophys. J. **572**, 996 (2002).

[5] S. Zane, R. Turolla, and J. J. Drake, astro-ph/0302197.

[6] C. Alcock, E. Farhi, and A. Olinto, Astrophys. J. **310**, 261 (1986); P. Haensel, J. L. Zdunik, and R. Schaeffer, Astron. Astrophys. **160**, 121 (1986).

[7] N. K. Glendenning, Compact Stars (Springer, New York, 1996).

[8] C. Y. Ng, K. S. Cheng, and M. -C. Chu, Astropart. Phys. **19**, 171 (2003).

[9] V. V. Usov, Phys. Rev. Lett. **80**, 230 (1998).

[10] V. V. Usov, Astrophys. J. **550**, L179 (2001).

[11] D. Page and V. V. Usov, Phys. Rev. Lett. **89**, 131101 (2002).

[12] See, for example, E. V. Shuryak, The QCD Vacuum, Hadrons and the Superdense Matter (World Scientific, Singapore, 1988), and references therein.

[13] K.-W. Wong and M.-C. Chu, Mon. Not. R. Astron. Soc. **350**, L42 (2004).

[14] Albert G. Petschek, Supernovae (Springer, New York, 1990).

[15] Z. Fodor and S. D. Katz, J. High Energy Phys. 03 (2002) 014.

[16] C. R. Allton et al., Phys. Rev. D **66**, 074507 (2002).

[17] O. G. Benvenuto and G. Lugones, Mon. Not. R. Astron. Soc. **304**, L25 (1999).

[18] F. Lebrun et al., Nature (London) **428**, 293 (2004).

[19] D. H. Oaknin and A. R. Zhitnitsky, hep-ph/0406146.

[20] D. N. Aguilera, D. Blaschke, and H. Grigorian, Astron. Astrophys. **416**, 991 (2004).

[21] E. S. Fraga, R. D. Pisarski, and J. Schaffner-Bielich, Phys. Rev. D **63**, 121702 (2001).

[22] B. Freedman, and L. McLerran, Phys. Rev. D **17**, 1109 (1978).

[23] V. Baluni, Phys. Rev. D **17**, 2092 (1978).

[24] F. Weber, Pulsars as Astrophysical Laboratories for Nuclear and Particle Physics (Institute of Physics, Bristol, 1999).

[25] E. Farhi and R. L. Jaffe, Phys. Rev. D **30**, 2379 (1984).

[26] K. W. Wong, MPhil thesis, Chinese University, 2003 (unpublished).

[27] K. Rajagopal and F. Wilczek, Phys. Rev. Lett. **86**, 3492 (2001).

[28] G. X. Peng, H. C. Chiang, P. Z. Ning, and B. S. Zhou, Phys. Rev. C **59**, 3452 (1999).

[29] J. Madsen, Phys. Rev. Lett. **85**, 4687 (2000).

[30] K. S. Cheng and Z. G. Dai, Phys. Rev. Lett. **77**, 1210 (1996).

[31] K. S. Cheng and Z. G. Dai, Phys. Rev. Lett. **80**, 18 (1998).

[32] I. Bombaci and B. Datta, Astrophys. J. **530**, L69 (2000).

[33] D. K. Srivastava and B. Sinha, Phys. Rev. Lett. **73**, 2421 (1994).

[34] A. C. Phillips, The Physics of Stars (John Wiley and Sons, New York, 1994).

[35] E. H. Gudmundsson, C. J. Pethick, and R. I. Epstein, Astrophys. J. **272**, 286 (1983).

[36] N. Iwamoto, Phys. Rev. Lett. **44**, 1637 (1980).

[37] A. Ipp, A. Gerhold, and A. Rebhan calculated the non-Fermi-liquid behavior of the specific heat, which is larger than that of the ideal case [Phys. Rev. D **69**, 011901 (2004)]. If this is the case, the cooling of the quark star will be slower.

[38] J. E. Horvath, O. G. Benvenuto, and H. Vucetich, Phys. Rev. D **44**, 3797 (1991).

[39] O. V. Maxwell, Astrophys. J. **231**, 201 (1979).

[40] L. P. Csernai, *Introduction to Relativistic Heavy Ion Collisions* (Wiley, New York, 1994).

[41] B. Muller and J. M. Eisenberg, Nucl. Phys. **A435**, 791 (1985).

[42] K. S. Cheng and T. Harko, Astrophys. J. **596**, 451 (2003).

[43] J. M. Lattimer, C. J. Pethick, M. Prakash, and P. Haensel, Phys. Rev. Lett. **66**, 2701 (1991).

[44] G. G. Festa and M. A. Ruderman, Phys. Rev. **180**, 1227 (1969).

[45] L. Lindblom, B. J. Owen, and G. Ushomirsky, Phys. Rev. D **62**, 084030 (2000).

[46] N. A. Gentile, M. B. Aufderheide, G. J. Mathews, F. D. Swesty, and G. M. Fuller, Astrophys. J. **414**, 701 (1993).

[47] A. G. Aksenov, M. Milgrom, and V. V. Usov, Mon. Not. R. Astron. Soc. **343**, L69 (2003).

[48] A. G. Aksenov, M. Milgrom, and V. V. Usov, Astrophys. J. **609**, 363 (2004).

[49] S. Tsuruta, Phys. Rep. **292**, 1 (1998).

[50] K. Hirata *et al.*, Phys. Rev. Lett. **58**, 1490 (1987).

[51] J. S. Bloom *et al.*, Nature (London) **401**, 453 (1999).

[52] J. N. Reeves *et al.*, Nature (London) **416**, 512 (2002).

[53] E. Waxman *et al.*, Nature (London) **423**, 388 (2003).